PHYSICAL REVIEW D **71,** 063523 (2005)

Observational constraints on interacting quintessence models

Germań Olivares*
Departamento de Física, Universidad Autónoma de Barcelona, Spain

Fernando Atrio-Barandela†
Departamento de Física Teórica, Universidad de Salamanca, Spain

Diego Pavón‡
Departamento de Física, Universidad Autónoma de Barcelona, Spain

(Received 13 September 2004; revised manuscript received 22 February 2005; published 22 March 2005)

We determine the range of parameter space of an Interacting Quintessence Model that best fits the recent WMAP measurements of Cosmic Microwave Background temperature anisotropies. We only consider cosmological models with zero spatial curvature. We show that if the quintessence scalar field decays into cold dark matter at a rate that brings the ratio of matter to dark energy constant at late times, the cosmological parameters required to fit the CMB data are: dark energy density $\Omega_x = 0.43 \pm 0.12$, baryon fraction $\Omega_b = 0.08 \pm 0.01$, slope of the matter power spectrum at large scales $n_s = 0.98 \pm 0.02$ and Hubble constant $H_0 = 56 \pm 4$ km/s/Mpc. The data prefers a dark energy component with a dimensionless decay rate parameter $c^2 = 0.005$ and noninteracting models are consistent with the data only at the 99.9% confidence level. Using the Bayesian Information Criteria we show that this extra parameter fits the data better than models with no interaction. The quintessence equation of state parameter is less constrained; i.e., the data sets an upper limit $w_x \leq -0.86$ at the same level of significance. When the WMAP anisotropy data are combined with supernovae data, the density parameter of dark energy increases to $\Omega_x \simeq 0.68$ while c^2 augments to 6.3×10^{-3}. Models with quintessence decaying into dark matter provide a clean explanation for the coincidence problem and are a viable cosmological model, compatible with observations of the CMB, with testable predictions. Accurate measurements of baryon fraction and/or of matter density independent of the CMB data, would support/disprove these models.

DOI: 10.1103/PhysRevD.71.063523 PACS numbers: 98.80.Es, 98.80.Bp, 98.80.Jk

I. INTRODUCTION

The recent observations of high redshift supernovae [1], Cosmic Microwave Background (CMB) temperature anisotropies [2] and the shape of the matter power spectrum [3] consistently support the idea that our Universe is currently undergoing an epoch of accelerated expansion [4]. Currently, the debate is centered on when did the acceleration actually start and what agent is driving it. A variety of models based on at least two matter components (baryonic and dark) and one dark energy component (with negative pressure) have been suggested—see [5]. The ΛCDM model, where a vacuum energy density or cosmological constant provides the negative pressure, was the earliest and simplest to be analyzed. While this model is consistent with the observational data (high redshift supernova [1], CMB anisotropies [2,6], galaxy cluster evolution [3]), at the fundamental level it fails to be convincing. The vacuum energy density falls below the value predicted by any sensible quantum field theory by many orders of magnitude [7], and it unavoidably leads to the *coincidence problem*, i.e., ''Why are the vacuum and matter energy densities of precisely the same order today?'' [8]. More sophisticated models replace Λ by a dynamical dark energy either in the form of a scalar field (quintessence), tachyon field, phantom field or Chaplygin gas. These models fit the observational data but it is doubtful that they solve the coincidence problem [9].

Recently, it has been proposed that dark matter and dark energy are coupled and do not evolve separately [10–17]. In particular the Interacting Quintessence (IQ) models of references [10–13], aside from fitting rather well the high redshift supernovae data, quite naturally solve the coincidence problem by requiring the ratio of matter and dark energy densities to be constant at late times. The coupling between matter and quintessence is either motivated by high energy particle physics considerations [10] or is constructed by requiring the final matter to dark energy ratio to be stable against perturbations [12,13]. Since the nature of dark matter and dark energy are unknown there are no physical arguments to exclude their interaction. On the contrary, arguments in favor of such interaction have been suggested [14]. As a result of the interaction, the matter density drops with the scale factor $a(t)$ more slowly than a^{-3}.

A slower matter density evolution fits the supernovae data as well as the ΛCDM concordance model does [13]. The interaction also alters the age of the Universe, the

*E-mail address: german.olivares@uab.es
†E-mail address: atrio@usal.es
‡E-mail address: diego.pavon@uab.es

evolution of matter and radiation perturbations and gives rise to a different matter and radiation power spectra. All these effects will be used to set constraints on the decay rate of the scalar field using cosmological observations. In this paper, we shall further constrain the Chimento *et al.* [13] model by using the recently WMAP measurements of the cosmic microwave background temperature anisotropies. As it turns out, a small but nonvanishing interaction between dark matter and dark energy is compatible with the WMAP data with the advantage of solving the coincidence problem. To some extent, this was already suggested in a recent analysis that uses the position of the peaks and troughs of the CMB [18] to constrain a general class of interacting models designed not to strictly solve the coincidence problem, but to alleviate it [19]. Briefly, the outline of the paper is: in Sec. II we summarize the cosmological model, in Sec. III we derive the equations of dark matter and dark energy density perturbations and find the range of parameter space that best fits the observations. Finally, in Sec. IV we discuss our main results and present our conclusions.

II. THE INTERACTING QUINTESSENCE MODEL

The IQ model considered here has been constructed to solve the coincidence problem by introducing a coupling between matter and dark energy; their respective energy densities do not evolve independently. In this paper, we shall simplify the Chimento *et al.* model [13] in the sense that the IQ will be assumed to decay into cold dark matter (CDM) and not into baryons, as required by the constraints imposed by local gravity measurements [5,20] The baryon-photon fluid evolves independently of the CDM and quintessence components. Unlike [13], we do not include dissipative effects. In [13] this scaling was considered only during matter domination, so the scalar field would evolve independently of the CDM component until it started to decay at some early time. These assumptions facilitate the numerical work while they preserve its essential features. Specifically, the quintessence field (denoted by a subscript x) decays into pressureless CDM (subscript c) according to [13]

$$\frac{d\rho_c}{dt} + 3H\rho_c = 3Hc^2(\rho_c + \rho_x),$$
$$\frac{d\rho_x}{dt} + 3(1 + w_x)H\rho_x = -3Hc^2(\rho_c + \rho_x), \tag{1}$$

where $w_x < 0$ is the equation of state parameter of the dark energy and c^2 is a small dimensionless constant parameter that measures the intensity of the interaction. Approaches similar (but not identical) to ours have been discussed in [10,11,15–17]. Eqs. (1) were not derived assuming some particle physics model for the interaction, where quintessence is described as an scalar field with a given potential. We followed a phenomenological approach and instead we have required the Interacting Quintessence Model to solve the coincidence problem. We have imposed the dark matter to dark energy density interaction to give a dark matter to dark energy ratio constant at late times and stable against perturbations. As a result, the shape of the scalar field potential is also fixed.

Eqs. (1) can be solved by Laplace transforming the system. The result is

$$\rho_x(a) = \frac{H_0^2}{8\pi G w_{\rm eff}}[3(c^2\Omega_{c,0} - (1 - c^2)\Omega_{x,0})(a^{S_+} - a^{S_-}) + \Omega_{x,0}(S_- a^{S_-} - S_+ a^{S_+})],$$
$$\rho_c(a) = \frac{H_0^2}{8\pi G w_{\rm eff}}[3((1 + w_x + c^2)\Omega_{c,0} + c^2\Omega_{x,0}) \times (a^{S_-} - a^{S_+}) + \Omega_{c,0}(S_- a^{S_-} - S_+ a^{S_+})], \tag{2}$$

where $w_{\rm eff} = (w_x^2 + 4c^2 w_x)^{1/2}$, and $S_\pm = -3(1 + w_x/2) \mp (3/2)w_{\rm eff}$. The density parameters $\Omega_{c,0}$ and $\Omega_{x,0}$ denote the current values of matter and dark energy, respectively. Solutions of Eqs. (1) are plotted in Fig. 1. Solid, dashed, dotted and dot-dashed lines correspond to Ω_c, Ω_x, Ω_r and Ω_b, respectively. In panel (a) $c^2 = 0.1$ and there is a short period of baryon dominance; this does not happen in panel (b) where $c^2 = 5 \times 10^{-3}$. As detailed in Ref. [13], the interaction dark matter–dark energy brings the ratio

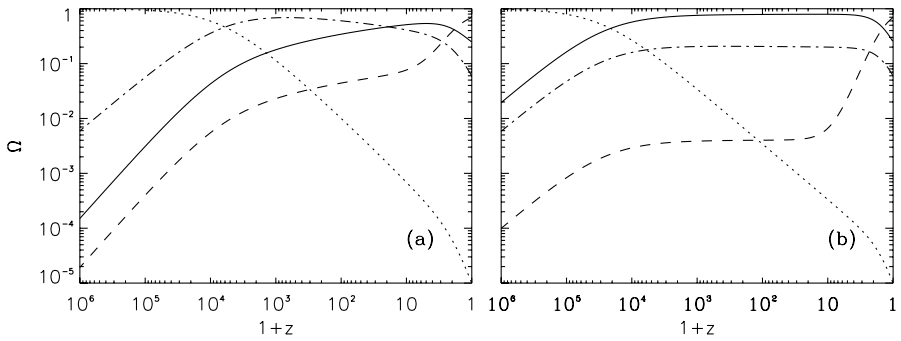

FIG. 1. Redshift evolution of different energy densities. Solid, dashed, dotted and dot-dashed lines correspond to Ω_c, Ω_x, Ω_r and Ω_b, respectively. In panel (a) $c^2 = 0.1$, and in panel (b) $c^2 = 5 \times 10^{-3}$. The following parameters were assumed: $\Omega_{c,0} = 0.25$, $\Omega_{x,0} = 0.7$, $\Omega_{b,0} = 0.05$, $\Omega_{r,0} = 10^{-5}$, and $w_x = -0.99$.

$r \equiv \rho_c/\rho_x$ to a constant, stable value at late times. From Eqs. (1), it is seen that the evolution of the aforesaid ratio is

$$\frac{dr}{dt} = 3Hc^2\left[r^2 + \left(\frac{w_x}{c^2} + 2\right)r + 1\right]. \tag{3}$$

The equation $dr/dt = 0$, has two stationary solutions, namely,

$$r_\pm = -w_x/(2c^2) - 1 \pm [w_x^2/(4c^4) + w_x/c^2]^{1/2},$$

which verify $r_+ r_- = 1$ (with $r_+ > r_-$). As shown in Fig. 2, the ratio evolves from an unstable maximum r_+ at early times—with dark matter and quintessence energy densities scaling as a^{S_+}- to a stable minimum r_- at late times, where both energy densities scale as a^{S_-}. In Fig. 2, the smaller the coupling constant the larger the ratio of cold dark matter to dark energy in the past and the smaller in the future without significantly affecting the length of the transition period. We are not suggesting that the Universe is already in the late time epoch of constant, stable ratio r_-. The value of the asymptotic ratio is determined by the strength of the interaction and at present this ratio could be still slowly evolving in time.

In terms of a scalar field description, the second equation of (1) is equivalent to

$$\frac{d^2\phi}{dt^2} + 3H\frac{d\phi}{dt} + V'_{\rm eff} = 0, \tag{4}$$

where ϕ denotes the dark energy field and $V_{\rm eff}(\phi)$ is the effective potential. The latter is given by

$$V'_{\rm eff} = \frac{dV(\phi)}{d\phi} + 3Hc^2(\rho_c + \rho_x)/(d\phi/dt). \tag{5}$$

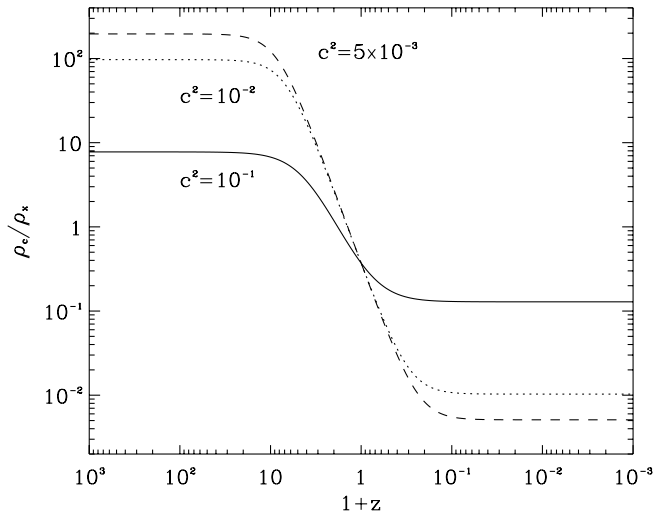

FIG. 2. Evolution of the ratio $r = \rho_c/\rho_x$ from an unstable maximum toward a stable minimum (at late times) for different values of c^2. We took $r_0 = 0.42$ as the current value.

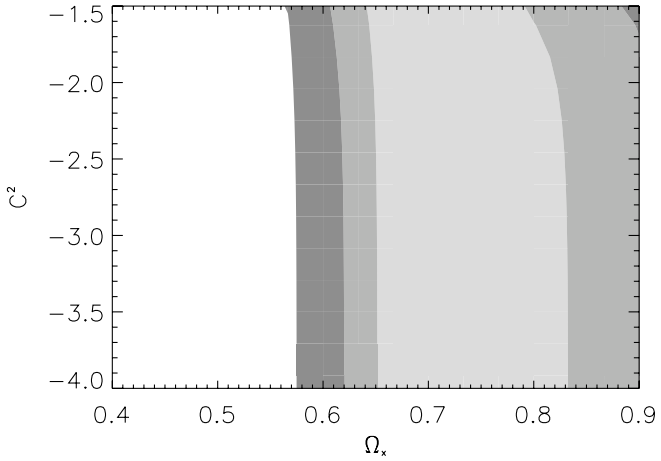

FIG. 3. Joint confidence intervals at 68%, 95% and 99.9% confidence level of IQM fitted to the "gold" sample of SNIa data of Riess *et al.* [1]

If $r =$ constant, the potential has two asymptotic limits: $V \propto e^{(-\phi)}$ during both matter domination and the period of accelerated expansion, and $V \propto \phi^{-\alpha}$ with $\alpha > 0$ well within the radiation dominated period. A detailed study has shown that only potentials that are themselves power laws—with positive or negative powers—or exponentials of the scalar field yield energy densities evolving as power laws of the scale factor [21]. Potentials with exponential and power-law behavior have been considered extensively in the high energy physics literature. Exponential potentials arise as a consequence of Kaluza-Klein type compactifications of string theory and in $N = 2$ supergravity while inverse power-law models arise in SUSY QCD (see [12,22]). Potentials showing both asymptotic behaviors have also been studied [23], but at present there are not satisfactory particle physics model to justify the shapes of potentials of this type [24].

From the evolution of the background energy densities it is possible to constrain the amplitude of the IQ and CDM coupling. Since $w_{\rm eff} > 0$, c^2 is confined to the interval $0 \leq c^2 < |w_x|/4$. Negative values of c^2 would correspond to a transfer of energy from the matter to the quintessence field and might violate the second law of thermodynamics. Further constraints can be derived by imposing stability of the interaction to first order loop corrections [25]. In Fig. 3 we used the supernova data of Riess *et al.* [1] to constrain model parameters. In the figure we plot the 68%, 95% and 99.9% confidence levels of a cosmological model after marginalizing over, w_x and the absolute magnitude of SNIa. We set a prior: $-1.0 \leq w_x \leq -0.6$. Variations of the baryon density produce no significant differences and the Hubble constant is unconstrained by this Hubble test since the absolute luminosity of Type Ia supernovae is not accurately measured. The contours are rather parallel to the c^2 axis, i.e., the low redshift evolution of interacting models is not very different from the noninteracting ones.

III. OBSERVATIONAL CONSTRAINTS ON THE MATTER-QUINTESSENCE COUPLING

Primordial nucleosynthesis and Cosmic Microwave Background temperature anisotropies provide the best available tools to constrain the physics of the early Universe. By assumption, the scalar field decays into dark matter and not into baryons. Since dark matter and quintessence density perturbations are coupled to baryon and photons only through gravity, there is no transfer of energy or momentum from the scalar field to baryons or radiation. The evolution of density perturbations of dark matter and dark energy can be simply derived from the energy conservation equation. In the equations below we shall use the conventions of [26]. In the synchronous gauge,

$$\dot{\delta}_c = -\frac{\dot{h}}{2} - 3\frac{\dot{a}}{a}c^2\left(\frac{\delta_x}{r} + \delta_c\right), \qquad \dot{\theta}_c = 0, \tag{6}$$

while the evolution of dark energy density perturbations is given by

$$\begin{aligned}\dot{\delta}_x &= -(1+w_x)\left(\theta_x + \frac{\dot{h}}{2}\right) - 3\frac{\dot{a}}{a}(c_s^2 - w_x)\delta_x \\ &\quad - 9\left(\frac{\dot{a}}{a}\right)^2(c_{s,x}^2 - w_x)(1+w_x)\theta_x k^{-2} + 3\frac{\dot{a}}{a}c^2(\delta_x + r\delta_c) \\ \dot{\theta}_x &= -(1-3c_{s,x}^2)\frac{\dot{a}}{a}\theta_x + \frac{k^2 c_{s,x}^2}{1+w_x}\delta_x \\ &\quad - 3\frac{\dot{a}}{a}\frac{c^2}{1+w_x}(1+r)\theta_x,\end{aligned} \tag{7}$$

where δ and θ denote the density contrast and the divergence of the peculiar velocity field of each component, respectively, derivatives are with respect to conformal time and $c_{s,x}^2$ is the quintessence sound speed, taken to be unity as for a scalar field with a canonical Lagrangian. The interaction introduces the terms with a c^2 factor on the right hand side of Eqs. (6) and (7). Combining these equations, the evolution of density perturbations in the IQ field are described by a driven damped harmonic oscillator, where the driving term is the gravitational field [27]. After a brief transient period, the evolution is dominated by the inhomogeneous solution and is insensitive to the initial amplitude. To find the model that best fits the WMAP data, we have implemented Eqs. (2), (6), and (7) into the CMBFAST code [28]. We used the likelihood code provided by the WMAP team [29] to determine the quality of the fit of every model to the data. Since we are introducing a new parameter, the coupling between dark matter and dark energy, the parameter space could become degenerate with different local maxima representing models that fit the data equally well. For this reason, we did not use a Monte Carlo Markov Chain approach [29] but we run through a grid of models on a six-dimensional parameter space. Grids of models are computationally very expensive. To make the computations feasible we reduced the parameter space by introducing prior information. We imposed two constraints: (i) all models were within the 90% confidence level of the constraint imposed by Big Bang Nucleosynthesis: $0.017 \leq \Omega_b h^2 \leq 0.027$ [30] and (ii) in all cosmologies the age of the Universe was chosen to be $t_0 > 12$ Gyr. With these requirements, we explore the region of parameter space close to the concordance model. We have considered only flat models with no reionization, no gravitational waves and no running of the spectral index. We considered a 6-dimensional parameter space and assumed our parameters to be uniformly distributed in the following intervals: Hubble constant $H_0 = [46, 90]$ km/s/Mpc, baryon fraction $\Omega_b = [0.01, 0.12]$, dark energy $\Omega_x = [0.1, 0.9]$, slope of the matter power spectrum on large scales $n_s = [0.95, 1.04]$, dark energy equation of state $w_x = [-1.0, -0.65]$ and $c^2 = [0, 0.05]$. We took 23, 15, 33, 10, 9 linear subdivisions and 22 logarithmic subdivisions of the above intervals, respectively. The likelihood was computed using the routines made publicly available by the WMAP team.

In Fig. 4 we give confidence intervals for pairs of parameters after marginalizing over the rest. Contours represent the 68%, 95% and 99.9% confidence levels. Models with $c^2 = 0$ have been computed and were included in the analysis. The results were undistinguishable from those of $c^2 = 10^{-4}$ the last point included in the graphs. The WMAP data sets strong upper limits on the quintessence decay rate. A nonzero decay rate is clearly favored by the data. At $c^2 \sim 10^{-2}$ the contours indicate a steep gradient in the direction of growing c^2. This behavior is associated with the decreasing fraction of CDM at recombination with increasing c^2. When the interaction rate is large, the Universe goes through a period dynamically dominated by baryons (Fig. 1(a)). The oscillations on the baryon-photon plasma induce large anisotropies in the radiation and those models are strongly disfavored by the data. In Fig. 4, the models fit the data more comfortably with lower values of Ω_x and H_0 than in the ΛCDM concordance model. Interacting models have larger dark energy density in the past than noninteracting models, achieving the same rate of accelerated expansion today with a smaller $\Omega_{x,0}$. Our best model also requires larger baryon fraction since the matter density is smaller prior to recombination than in the concordance model, therefore dark matter potential wells are shallower and a higher baryon fraction is required to reproduce the amplitude of the first acoustic peak [31]. The mean value of the cosmological parameters and their corresponding 1σ confidence intervals are: $\Omega_x = 0.43 \pm 0.12$, $\Omega_b = 0.08 \pm 0.01$, $n_s = 0.98 \pm 0.2$ and $H_0 = 56 \pm 4$ km/s/Mpc. The latter number is not very meaningful since the probability distribution of H_0 is rather skewed. As it can be seen in Fig. 4(a), low values of H_0 are suppressed very fast. As the height of the first acoustic peak scales with $\Omega_b h^2$, high values of baryon

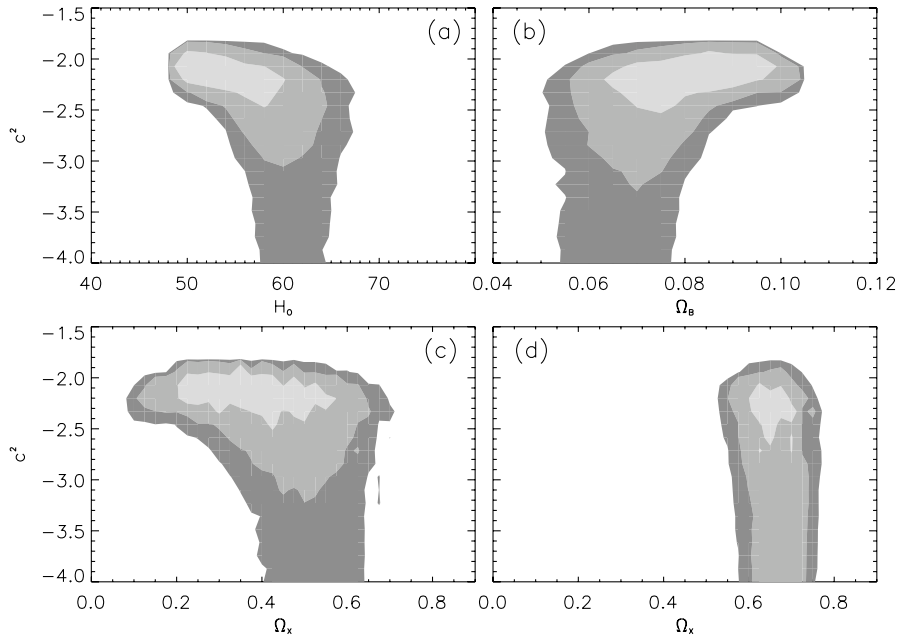

FIG. 4. Joint confidence intervals at the 68%, 95% and 99.9% level for pairs of parameters after marginalizing over the rest. For convenience the c^2 axis is represented using a logarithmic scale and it has been cut to $c^2 \leq 10^{-4}$, though models with $c^2 = 0$ have been included in the analysis. In panels (a), (b) and (c) models were fit to CMB data alone. In panel (d) we included supernovae data of Riess *et al.* [1].

fraction are speedily suppressed by the WMAP data, which translates into an even faster suppression of low values of H_0. With respect the quintessence equation of state, as we did not explore models with $w_x < -1$, we can only set an upper limit $w_x \leq -0.86$ at the 1σ confidence level. Finally, as we chose a uniform prior on $\log c$, the confidence interval is not symmetric, resulting: $c^2 = 0.005^{+0.007}_{-0.003}$.

Our main result is that models with interaction are preferred over noninteracting models, with the remarkable feature that they require very different cosmological parameters than the concordance model. The range for Ω_x, H_0, Ω_b and w_x are not directly comparable to those found in [10] since the interaction is different and we used different priors. Their coupled model requires higher values of the Hubble constant when the strength of the interaction increases, opposite to the behavior found in Fig. 4. Noninteracting models are compatible with the data only at the 99.9% confidence level. Our best fit model ($c^2 = 5 \times 10^{-3}$, $\Omega_x = 0.43$, $\Omega_b = 0.08$, $H_0 = 54$ km/s/Mpc, $n_s = 0.98$, $w = -0.99$) has a $\chi^2 = -2\log(\mathcal{L}) = 974$ while the best fit for a noninteracting model occurs at $\Omega_x = 0.5$, $\Omega_b = 0.07$, $H_0 = 60$ km/s/Mpc, $w = -0.75$, $n_s = 1.02$ and has $\chi^2 = 983$. The Bayesian Information Criteria defined as $BIC = \chi^2 + k \log N$ [32], that penalizes the inclusion of additional parameters to describe data of small size (in this case the number of independent data points is $N = 899$ and k, the number of model parameters, is 5 in the non-IQ model, and 6 in the model with interaction), gives $\Delta BIC = -2$ which can be considered as positive evidence in favor of including this additional parameter to describe the data. The ΛCDM concordance model was deduced by fitting a different set of parameters to WMAP data [29] and the results are not directly comparable to ours. For completeness, let us mention that the concordance model with $\Omega_\Lambda = 0.72$, $\Omega_b = 0.049$, $H_0 = 68$ Km/s/Mpc and $n_s = 0.97$ has a fit of $\chi^2 = 972$ is positively better than ours if the amplitude of the matter power spectrum and the redshift of reionization are included as parameters. If only the overall normalization of the power spectrum is included, the fit is $\chi^2 = 990$. In this case, the BIC would give $\Delta BIC = -9$ that must be taken as strong indication that the interaction improves the fit.

The likelihood curves of Fig. 4 seems to suggest that our model is ruled out by observations since, for example, luminosity distance estimates from high redshift supernovae indicate that $\Omega_x \geq 0.6$ at the 95% confidence level [1]. However, analysis of the temperature-luminosity relation of distant clusters observed by XMM-Newton and Chandra satellites appear to be consistent with Ω_c up to 0.8 [33]. Moreover, with no priors on Ω_c and w_x, (so phantom models are included in the analysis) values of the CDM fraction as high as ours are consistent with SNIa data [34]. Contours in Fig. 4(c) are rather parallel to the Ω_x-axis, while at the redshifts probed by supernovae interacting models behave as noninteracting, and in the same plane contours are parallel to the c^2-axis (see Fig. 3). In Fig. 4(d) we plot the confidence intervals combining both WMAP and high redshift supernovae data. Contours are shifted to large values of dark energy, the reason being that WMAP

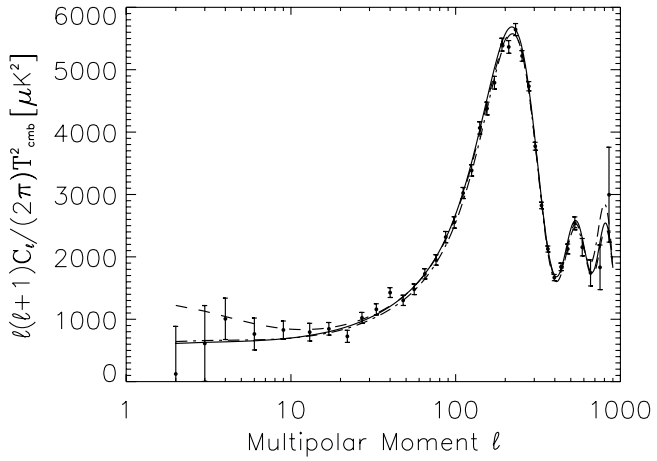

FIG. 5. Radiation Power Spectrum. The solid line is our best fit model ($c^2 = 5 \times 10^{-3}$, $\Omega_x = 0.43$, $\Omega_b = 0.08$, $H_0 = 54$ km/s/Mpc, $n_s = 0.98$,$w = -0.99$). Dashed line corresponds to the ΛCDM concordance model and dot-dashed line is $QCDM$ with parameters $\Omega_x = 0.5$, $\Omega_b = 0.07$, $H_0 = 60$ km/s/Mpc, $w = -0.75$ and $n_s = 1.02$.

data constraints the coupling c^2 while the supernovae data is insensitive to it. For illustrative purposes, in Fig. 5 we compare our best fit model (solid line) with the concordance model (dashed line) and the best quintessence model with $c^2 = 0$ (dot-dashed). All models are rather smooth compared with the rigging present in the data with the excess χ^2 coming from similar regions in l-space: $l \sim 120, 200, 350$. The discrepancy among the models is clearer at the first acoustic peak. This rigging introduces a high degeneracy among cosmological parameters since very different models fit the data with similar χ^2 per degree of freedom. When adding other data sets, like the supernovae in Fig. 4(c), the fraction of dark energy increases dramatically. With respect to the Hubble constant, the value is less certain since several groups advocate values close to 60 km/s/Mpc [35], and even as low as 50 km/s/Mpc [36].

There is a significant difference between the concordance model and our best fit model. Since the latter requires lower Hubble constant and dark energy density, it generates a smaller Integrated Sachs Wolfe effect, responsible for the rise of the radiation power spectrum at $l \leq 10$. This is a generic feature of this type of IQ models and, therefore, the low amplitude of the measured quadrupole and octupole is less of a problem in models with decaying dark energy than in the concordance model.

IV. DISCUSSION

We have shown that a model where the coincidence problem is solved by the decay of the quintessence scalar field into cold dark matter is fully compatible with the WMAP data. The best model, $c^2 \simeq 5 \times 10^{-3}$, fits the data significantly better than models with no interaction. Our best fit model requires cosmological parameters, in particular Ω_x and H_0, that are very different from the concordance model. Our models are highly degenerate in the $\Omega_x - c^2$ plane with contours almost parallel to the Ω_x axis (see Fig. 4) but including prior information from supernovae data shifts this parameter close to the concordance model $\Omega_x \simeq 0.68$. We wish to emphasize that the noninteracting model ($c^2 = 0$) is only compatible with WMAP data at 3σ confidence level, but when the supernovae data are included this is shifted to 2σ confidence level.

We have shown that the Bayesian Information Criteria, that strongly disfavors increasing the parameter space to describe data sets of $N \simeq 10^3$ points, provides positive evidence in favor of the existence of interaction. Other IQ models have been proposed [10] and even if their results are not directly comparable to ours, two interacting models, constructed with different motivations, suggest a value of the dark energy density smaller than in the concordance model, signals a need to investigate this type of models. As we have discussed, the quality of the fit and the cosmological parameters that can be derived by fitting cosmological models to observations depend on the parameter space explored.

The fact that IQ models appear to be favored by current observations suggests that dark energy and dark matter might not be so different entities after all. This is in line with recent ideas involving the Chaplygin gas. There, a single component plays the dual role of cold dark matter (at early times) and vacuum energy (at late times) and it interpolates between the two as expansion proceeds [37]. The matter power spectrum could also be an important test of IQ models. A preliminary study shows that for the range of parameter space compatible with WMAP, the effect of the scalar field decaying into CDM has little effect [38].

To summarize, the interacting cosmology model fits the WMAP data significantly better than the ΛCDM model does, and in fact alleviates the ISW effect at large angular scales, has no coincidence problem and provides a unified picture of dark matter and dark energy. It predicts lower values of Hubble constant, dark energy density and higher baryon fraction. It is to be expected that the next generation of CMB experiments [39] and large scale surveys will enable us to constrain c^2 even further and discriminate between the different variants.

ACKNOWLEDGMENTS

The authors wish to thank Alejandro Jakubi for discussions and comments. This research was partially supported by the Spanish Ministry of Science and Technology under Grants BFM2003-06033, BFM2000-1322 and AYA2000-2465-E and the Junta de Castilla y León (project SA002/03).

[1] S. Perlmutter *et al.*, Nature (London) **391**, 51 (1998); A. G. Riess *et al.*, Astrophys. J. **607**, 665 (2004).

[2] D. N. Spergel *et al.*, Astrophys. J. Suppl. Ser. **148**, 175 (2003).

[3] M. Tegmark *et al.*, Phys. Rev. D **69**, 103501 (2004).

[4] S. Carroll, in *Measuring and Modelling the Universe*, Carnegie Observatories Astrophysic Series, edited by W. L. Freedman (Cambridge University Press, Cambridge, 2004); T. Padmanbhan, Phys. Rep. **380**, 235 (2003); J. A. S. Lima, Braz. J. Phys. **34**, 194 (2004); V. Sahni, astro-ph/0403324; in *Proceedings of the I.A.P. Conference On the Nature of Dark Energ*, edited by P. Brax (Frontier Group, Paris, 2002); in *Proceedings of the IVth Marseille Cosmology Conference Where Cosmology and Fundamental Physics Meet, 2003*, edited by V. Lebrun, S. Basa and A. Mazure (Frontier Group, Paris, 2004).

[5] P. J. E. Peebles and B. Ratra, Rev. Mod. Phys. **75**, 559 (2003).

[6] P. D. Mauskopf *et al.*, Astrophys. J. **536**, L59 (2000).

[7] S. Weinberg, Rev. Mod. Phys. **61**, 1 (1989).

[8] P. J. Steinhardt, in *Critical Problems in Physics*, edited by V. L. Fitch and D. R. Marlow (Princeton University Press, Princeton, New Jersey, 1997).

[9] L. P. Chimento, A. S. Jakubi, and D. Pavón, Phys. Rev. D **62**, 063508 (2000); **67**, 087302 (2003).

[10] L. Amendola, Phys. Rev. D **62**, 043511 (2000); L. Amendola and D. Tocchini-Valentini, Phys. Rev. D **64**, 043509 (2001); L. Amendola and D. Tocchini-Valentini, Phys. Rev. D **66**, 043528 (2002); L. Amendola, C. Quercellini, D. Tocchini-Valentini, and A. Pasqui, Astrophys. J. **583**, L53 (2003).

[11] D. Tocchini-Valentini and L. Amendola, Phys. Rev. D **65**, 063508 (2002).

[12] W. Zimdahl, D. Pavón, and L. P. Chimento, Phys. Lett. B **521**, 133 (2001).

[13] L. P. Chimento, A. S. Jakubi, D. Pavón, and W. Zimdahl, Phys. Rev. D **67**, 083513 (2003).

[14] G. Farrar and P. J. E. Peebles, Astrophys. J. **604**, 1 (2004).

[15] B. M. Hoffman, astro-ph/9397359; G. Huey and B. D. Wandelt, astro-ph/0407196.

[16] G. Mangano, G. Miele, and V. Pettorino, Mod. Phys. Lett. A **18**, 831 (2003).

[17] Rong-Gen Cai and Anzhong Wang, hep-th/0411025.

[18] D. Pavón, S. Sen, and W. Zimdahl, J. Cosmol. Astropart. Phys. 05 (2004) 009.

[19] W. Zimdahl and D. Pavón, Gen. Relativ. Gravit. **35**, 413 (2003).

[20] K. Hagiwara *et al.*, Phys. Rev. D **66**, 010001 (2002).

[21] A. R. Liddle and R. J. Scherrer, Phys. Rev. D **59**, 023509 (1999).

[22] E. J. Copeland, N. J. Nunes, and F. Rosati, Phys. Rev. D **62**, 123503 (2000).

[23] V. Sahni and L. Wang, Phys. Rev. D **62**, 103517 (2000).

[24] P. Brax, J. Martin, and A. Riazuelo, Phys. Rev. D **62**, 103505 (2000).

[25] M. Doran and J. Jäckel, Phys. Rev. D **66**, 043519 (2002).

[26] C. P. Ma and E. Bertschinger, Astrophys. J. **455**, 7 (1995).

[27] R. Dave, R. R. Caldwell, and P. J. Steinhardt, Phys. Rev. D **66**, 023516 (2002).

[28] U. Seljak and M. Zaldarriaga, Astrophys. J. **469**, 437 (1996); see http://www.cmbfast.org.

[29] L. Verde *et al.*, Astrophys. J. Suppl. Ser. **148**, 195 (2003); G. Hinshaw *et al.*, Astrophys. J. Suppl. Ser. **148**, 135 (2003); A. Kogut *et al.*, Astrophys. J. Suppl. Ser. **148**, 161 (2003).

[30] K. Olive, astro-ph/0301505.

[31] W. Hu and S. Dodelson, Annu. Rev. Astron. Astrophys. **40**, 171 (2002).

[32] G. Schwarz, Ann. Statistics **5**, 461 (1978); A. R. Liddle, Mon. Not. R. Astron. Soc. **351**, L49 (2004).

[33] S. C. Vauclair *et al.*, Astron. Astrophys. **412**, L37 (2003).

[34] J. M. Virey, A. Ealet, C. Tao, A. Tilquin, A. Bonissent, D. Fouchez, and P. Taxil, Phys. Rev. D **70**, 121301 (2004).

[35] A. Blanchard *et al.*, Astron. Astrophys. **412**, 35 (2003); G. A. Tammann *et al.*, Astron. Astrophys. **404**, 423 (2003).

[36] E. S. Battistelli *et al.*, Astrophys. J. **598**, L75 (2003).

[37] A. Kamenschik, U. Moschella, and V. Pasquier, Phys. Lett. B **511**, 265 (2001); N. Bilic, G. B. Tupper, and R. D. Viollier, Phys. Lett. B **535**, 17 (2002); M. C. Bento, O. Bertolami, and A. A. Sen, Phys. Rev. D **66**, 043507 (2002).

[38] G. Olivares, F. Atrio-Barandela, and D. Pavón (work in progress).

[39] http://www.rssd.esa.int/index.php?project=PLANCK.